Journal of Naval Architecture and Marine Engineering
July, 2025
https://doi.org/10.3329/jname.v22i2.68153 http://www.banglajol.info

FINITE ELEMENT MODELLING OF NON-LINEAR THERMAL BUCKLING ANALYSIS OF DIFFERENT MULTILAYER OFFSHORE PIPELINES

R. Balan[1] and Vadivuchezhian Kaliveeran[2*]

[1]Department of Water Resources and Ocean Engineering, National Institute of Technology Karnataka, Mangalore 575025, India, balanmit@gmail.com

[2*]Department of Water Resources and Ocean Engineering, National Institute of Technology Karnataka, Mangalore 575025, India, vadivuchezhian_k@yahoo.co.in

Abstract:

Offshore pipelines operating under harsh environmental conditions of high temperature and pressure are susceptible to thermal buckling. The presence of initial imperfections in a pipeline significantly increases its susceptibility to global buckling failure when exposed to thermal stresses and internal pressure. This risk is further exacerbated by temperature gradients across the pipeline's wall, primarily driven by heat transfer between the petroleum products and the surrounding environment. This research utilizes the finite element (FE) analysis software ANSYS to investigate the effect of radial temperature gradients and initial imperfections on the thermal buckling behavior of various multilayer offshore pipeline designs, including lined, sandwich (SW), and pipe-in-pipe (PIP) configurations. The FE model employs a sequentially coupled analysis of heat transfer and nonlinear thermal buckling. Buckling temperatures are determined for each configuration and compared with those of a conventional single-layer (SL) pipeline. The impact of insulation on pipeline performance is assessed through an analysis of radial temperature and Von Mises stress profiles. The results demonstrated that the PIP configuration exhibited the most significant improvement in critical buckling temperature, surpassing both the single-layer and other multilayer pipelines. In contrast, the lined pipe's buckling temperature is nearly identical to that of the single-layer pipeline. The results further demonstrate that the buckling temperature of the multilayer pipelines is influenced by the temperature variation across the pipeline's radius, the properties of the insulation layers, and the initial imperfections of the pipelines.

Keywords: Multilayer pipelines, natural convection, imperfection, FE modeling, non-linear buckling

NOMENCLATURE

T	temperature	h_{ex}	external heat transfer coefficient
L	length	T_{cri}	critical buckling temperature
D	diameter	r_{in}, r_{ex}	internal and external radius
t	thickness	***Greek symbols***	
E	modulus of elasticity	ρ	density
k	thermal conductivity	μ	dynamic viscosity
c	specific heat capacity	α	thermal diffusivity
h_{in}	internal heat transfer coefficient	ν	Poisson's ratio

1. Introduction

Offshore pipelines are gaining popularity as a method of transporting oil and natural gas from oil rigs to resource storage places. This means of transportation is also known for its reliability, safety, and lower cost than other methods of transportation (Yu et al., 2022; Du et al., 2023; Zhang et al., 2018). The necessity of offshore oil and gas has increased because of the demand for it and the depletion of reserves. This has increased exploration in deep and ultra-deep reservoirs where severe conditions such as high temperature (up to 150°C) and pressure (up to 70 MPa) are encountered along with highly different properties (Leeuw et al., 2022; Shadravan and Amani, 2012; Zhang et al., 2018; Yang et al., 2024). One such problem is thermal buckling of pipelines, whether laid directly or buried under the seabed. The buckling is a nonlinear process which leads to a sharp deformation of the

1813-8535 (Print), 2070-8998 (Online) Received on: August, 2023

structure. This deformation may occur progressively without causing irreversible damage or substantially faster, as in catastrophic failure (Bracaglia et al., 2024).

During high-temperature operation, subsea pipelines have undergone thermal expansion, leading to a serious axial force on the pipeline's structure. However, the growth is limited by the friction on the seabed and the boundary conditions of the pipeline (Wang et al., 2020; Guo et al., 2013). As the critical axial force of the pipeline value is achieved, the compressive stress is released by buckling (Zhang et al., 2018; Guo et al., 2013). Global thermal buckling of offshore pipelines is classically divided into two categories: lateral buckling and upheaval buckling. Lateral buckling is common in free-span pipelines. This is where the pipeline is susceptible to lateral flexure because of low lateral restraint. In the case of buried or trenched pipelines, however, no lateral movement is possible, and the pipeline must uplift due to soil resistance, resulting in upheaval buckling (Wang et al., 2017; Ning et al., 2022; Liu et al., 2014). Consequences of buckling may be very serious, like permanent deformations, collapse, local deformations, fracture, and fatigue. Such accidents can be environmentally damaging and economically costly in terms of loss to oil and gas resources (Ning et al., 2022; Vazouras et al., 2021; Wang et al., 2023). It is necessary to take the concern of buckling into account in pipeline design as well in the following period for reconnaissance and maintenance (Xu and Lin, 2017).

The temperature differential between the petroleum products and the ambient seawater is considered as uniform in the thermal buckling studies for offshore pipelines (Liu et al., 2014; Hobbs, 1984; Vazouras et al., 2021). Nevertheless, relatively few studies have addressed thermal buckling due to changes in temperature distribution through the wall, considering steady-state and transient heat transfer analysis (Andreuzzi and Perrone, 2001; Wang et al., 2017). Heat transfer analysis is important in thermal analysis of offshore pipelines because it leads to the understanding of temperature distribution in the wall of a pipeline subjected to HP/HT conditions. The steady-state analysis is used to consider the long-term temperature distribution, whereas the transient analysis is necessary to understand the temperature fluctuations during pipeline in start-up and shutdown phases (Chakraborty et al., 2016; Tafreshi et al., 2015; Swain et al., 2023).

Once crude oil starts to circulate in the pipelines, it becomes cold as a result of heat transfer to the ambient seawater. This cooling by conduction and convection is capable of causing the oil to cool to its Wax Appearance Temperature (WAT) (Zhang et al., 2014; Aiyejina et al., 2011). When the oil cools down to this temperature, it thickens in the pipeline to wax. Waxes and hydrates deposition can severely hinder the pipeline operation (Park et al., 2020; Yu et al., 2024). To reduce these risks, suitable insulation means are provided to keep the oil above the WAT. In offshore pipeline systems in an HPHT environment, protection against wax and hydrate deposits is commonly done by the use of polymeric insulation. There are two approaches to heat loss control in order to keep the operation efficiency: passive control and active heating. Passive methods for control include the use of physical barriers to retard heat transfer out of the object, for example, by stacking layers of insulation or burying the pipe. Active heating methods also employed external sources of heat (electrical heating or hot fluid circulation) to elevate and sustain the temperature of the pipeline above the critical level (Kumar et al., 2022). Most of the research efforts on thermal buckling of offshore pipelines focused on single-layer pipelines, mainly via analytical, numerical, and experimental analyses (Hobbs, 1984; Guo et al., 2013; Liu et al., 2014; Taylor and Tran, 1996).

Single-layer pipelines are playing a more important role in the oil and gas exploitation of deep and ultra-deepwater field because of the growing requirement of petroleum resources and the development of pipeline technology to meet the severe conditions. In these pipelines, thicker pipe walls are required to resist cold temperature and high external pressure, therefore, material and installation costs are increased. In addition, these single-layer pipelines need a high operational cost to circulate hot fluids and avoid the formation of material like paraffin and hydrates (Wei et al., 2024). To cope with these problems, an alternative type of pipeline, i.e., multilayer pipeline, including PIP, SW, and lined pipelines, has been developed. Examples of multilayer pipelines used for offshore applications are shown in Fig. 1.

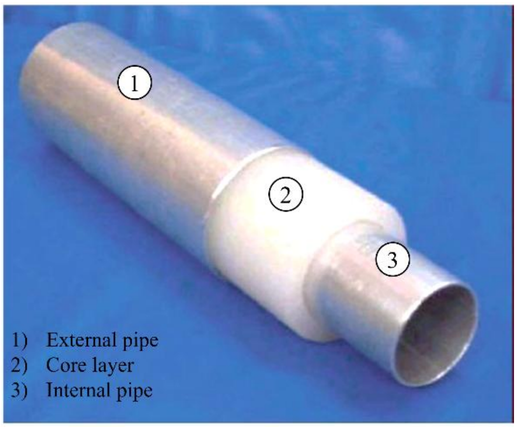

(a) Sandwich pipeline (Estefen et., 2005) (b) Unbonded flexible pipe (Cornacchia et al., 2019)

Fig. 1: Examples of multilayer pipelines

A PIP is assembled with two concentric steel tubes (Wei et al., 2024). There may be a circular space between these tubes (empty space) or it may be loaded with insulation material (Zhang et al., 2019). The inner pipe is used to transport petroleum products, and the outer pipe, known as a carrier, serves to protect the insulation against the environment (Wang et al., 2024). On the other hand, a SW pipeline includes a laminated or three-layered structure having a number of material layers bonded together to function as a pipeline. In PIP systems, the core material is non-structural; however, the core material used in SW pipelines has structural and thermal strength. SW pipelines present some advantages in relation to conventional SL pipelines, such as higher strength-to-weight ratio, lower production cost, and structural capacity, as well as an improved thermal insulation. These advantages make them quite desirable to address the rising challenges of deep-sea transportation (Chen et al., 2024; Song et al., 2022; Onyegiri and Kashtalyan, 2017). Lined pipe is a kind of multilayer pipeline and it is used as one of the cost-effective approaches to prevent the corrosion in oil and gas steel pipelines. The pipelines are comprised of an outer heavy-wall pipe, usually constructed of low-carbon steel, and an inner, much thinner walled lining, usually 2-3 millimeters thick, forged from a corrosion-resistant alloy. As a result of this structure, the pipeline will be safe from exposure to high temperatures generated during underwater burial, as well as will ensure the line’s safety against corrosive substances such as H2S, chlorides, and water, and the cost will be minimized since it will eliminate the need of expensive materials, such as SS or Ni alloys (Gavriilidis and Karamanos, 2019; Vedeld et al., 2012).

The past forty years have seen continuous development of computer techniques, which has made finite element analysis (FEA) a common tool to check offshore pipeline buckling. Pipe thermal buckling may be analyzed by two major approaches: linear eigenvalue buckling analysis and nonlinear analysis. The assumptions of small pre-buckling deformations are inherent in linear eigenvalue analysis. The detailed nature of these deformations and the ensuing load-carrying capacity of a buckled structure, however, are not well understood. In order to predict the buckling of pipelines with good accuracy, especially when buckling becomes an important issue, it is important to take geometric nonlinear effects into account (Liang et al., 2024). Commonly performed nonlinear buckling analyses are geometric nonlinearity analysis and a material nonlinearity analysis, or a combination. For instance, geometric non-linearity when combined with geometric imperfections leads to more realistic structural responses (Wagner and Huhne, 2024).

The objective of this study is to consider, by means of non-linear thermal buckling analysis, the effect of the radial temperature gradients and initial geometrical imperfections on the buckling temperature of multi-layer offshore pipelines. For the numerical analysis, four pipelines will be considered: single, PIP, SW, and lined. Temperature distributions on the pipelines were evaluated by conducting steady-state heat transfer analyses with ANSYS. Subsequently, the derived temperature profiles were incorporated in a linear eigenvalue buckling analysis. Furthermore, a nonlinear buckling analysis has been conducted to evaluate the realistic critical buckling temperature of all the pipelines considered above by using the linear buckling mode shapes as initial imperfections.

Finally, the buckling temperature of the multilayer pipeline was then compared with the buckling temperature of the single layer pipeline.

2. Formulation of the Problem

2.1 Problem definition

To evaluate the temperature profile across the pipeline's cross-sectional area, a steady-state heat transfer model was implemented.

The assumptions made in this study are outlined below

- The temperature profile within the pipeline is assumed to be time-invariant, varying only with the radial distance from the centerline.
- The temperature is considered constant along the axial direction of the pipeline.
- The influence of temperature on the material properties of the pipeline is neglected.
- The generation of heat within the pipeline is neglected
- Given the axisymmetric geometry of the pipeline and the assumed temperature distribution, the temperature at any point within the cross-section is solely a function of the radial coordinate.
- It is assumed that turbulence does not significantly influence heat transfer, which is neglected in this analysis.
- Radiative heat transfer is assumed to be negligible compared to conductive and convective heat transfer.
- The fluid within the pipe is considered incompressible, and it is assumed that no phase changes, such as evaporation or condensation, occur during the heat transfer process.
- The heat generation due to internal fluid friction and the temperature change associated with the Joule-Thomson effect are considered negligible.
- The thermophysical properties, such as thermal conductivity, specific heat capacity, and density, of each material layer, are assumed to remain unchanged over the temperature range considered.

The model, formulated in a 3D cylindrical coordinate system, is governed by the following differential equation (Janna, 2018):

$$\frac{1}{r}\frac{\partial}{\partial r}\left(r\frac{\partial T}{\partial r}\right)+\frac{1}{r^2}\frac{\partial^2 T}{\partial \theta^2}+\frac{\partial^2 T}{\partial z^2}+\frac{q}{k}=\frac{1}{\alpha}\frac{\partial T}{\partial t} \quad (1)$$

where k denotes the thermal conductivity, q signifies the heat generation, and α is the thermal diffusivity.
Based on the assumptions mentioned above, the heat transfer equation in a 3D cylindrical coordinate system can be simplified as follows:

$$\frac{1}{r}\frac{\partial}{\partial r}\left(r\frac{\partial T}{\partial r}\right)=0 \quad \text{or} \quad \frac{d}{dr}\left(r\frac{dT}{dr}\right)=0 \qquad \text{Since T is dependent on r} \quad (2)$$

Eq. (2) leads to the subsequent result:

$$T(r)=C_1\ln r+C_2 \quad (3)$$

where C_1 and C_2 represent integration constants, which are evaluated by applying the following boundary conditions. The interior and exterior walls of the pipeline are exposed to a convective boundary condition, as shown in Fig. 2, and these boundary conditions are expressed as:

$$\left(-k\frac{dT}{dr}\right)_{r=r_{in}}=h_{in}\left(T-T_{\infty 1}\right) \quad (4)$$

$$\left(-k\frac{dT}{dr}\right)_{r=r_{ex}}=h_{ex}\left(T-T_{\infty 2}\right) \quad (5)$$

where, $T_{\infty 1}$ and $T_{\infty 2}$ correspond to the temperatures of the crude oil and seawater, respectively; h_{in} and h_{ex} represent the convective heat transfer coefficients for the pipeline's internal and external surfaces; r_{in} and r_{ex} denote the inner and external radii of the pipelines. The temperature profile across the single-layer pipeline is obtained by applying the mixed boundary conditions into Eq. (3). The resulting temperature profile is expressed by Eq. (6).

$$T(r)=\frac{1}{\frac{k}{r_{in}h_{in}}+\ln\frac{r_{ex}}{r_{in}}+\frac{k}{r_{ex}h_{ex}}}\left\{\left[T_{ex}-T_{in}\right]\ln r+\left[T_{in}\ln r_{ex}-T_{ex}\ln r_{in}+\frac{k}{r_{ex}h_{ex}}T_{in}+\frac{k}{r_{in}h_{in}}T_{ex}\right]\right\} \quad (6)$$

Similarly, the radial temperature variation in multilayer pipelines can be calculated.

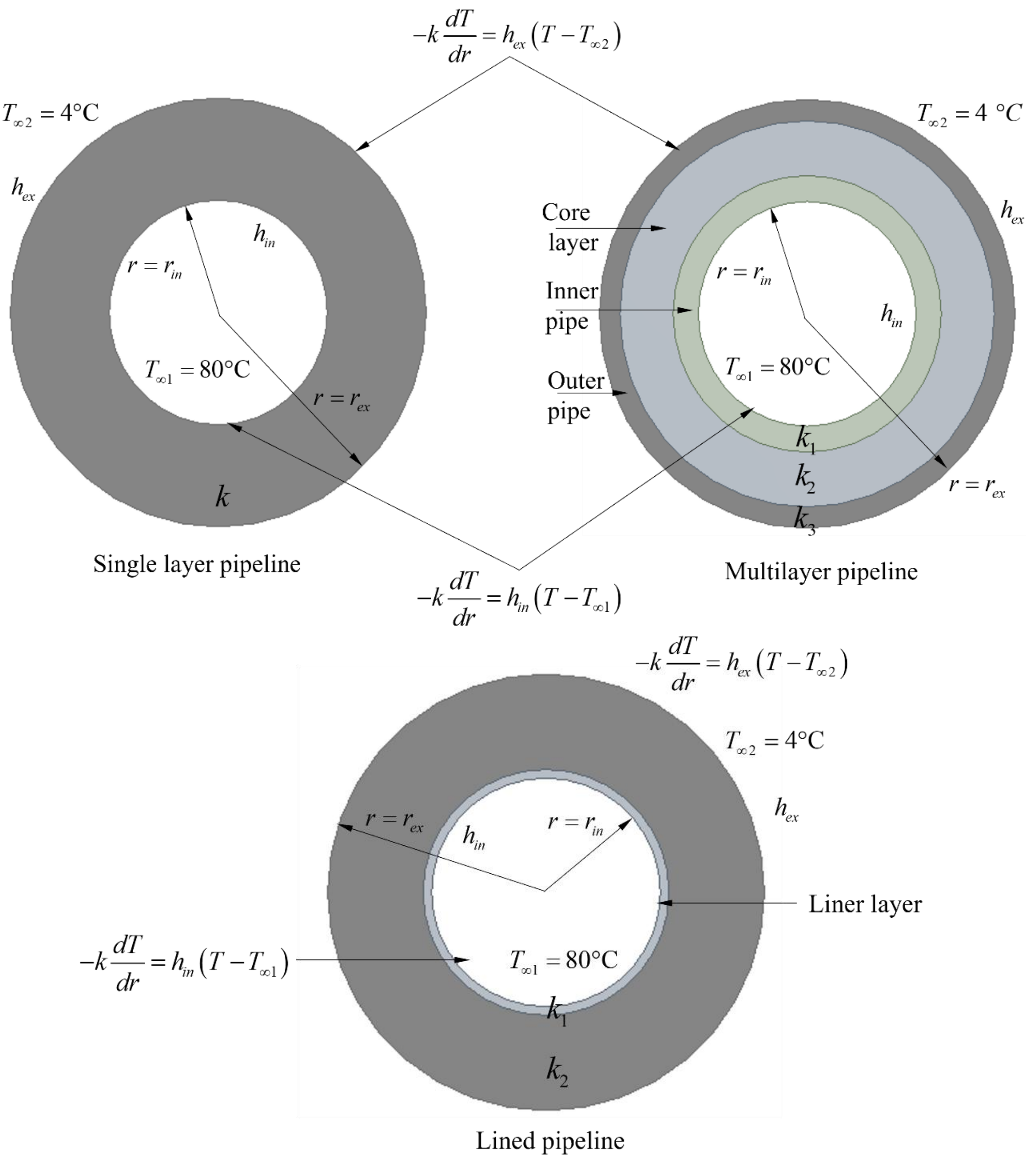

Fig. 2: Convective boundary conditions in single and multilayer pipelines

2.2 Material properties

Table 1 outlines the physical characteristics of seawater and crude oil. Both SW and PIP systems utilize API 5L-X65-grade steel for all pipe components, including the outer pipe of the lined pipeline. Table 2 summarizes the mechanical properties of this steel.

Table 1. Crude oil and seawater characteristics (Castello and Estefen 2008)

Parameter	Crude oil	Sea water
Temperature, T, °C	80	4
Density, ρ, (kg/m^3)	800	1025
Dynamic viscosity, μ, (Ns/m^2)	0.06712	0.00175
Thermal conductivity, k, (W/m °C)	0.14	0.57
Specific heat capacity, c, (kJ/kg °C)	2.7	4.217

Table 2. Pipeline dimensions and material characteristics (Wang et al., 2017; Castello and Estefen, 2008)

Property	Outer Pipe	Inner pipe	Liner	Polypropylene	Polyurethane
Diameter (m)	0.152	0.098	-	-	-
Thickness (m)	0.0076	0.0092	0.003	0.0194	0.0194
Density, ρ, (kg/m^3)	7800	7800	7800	893	700
Modulus of elasticity, E, (GPa)	206	206	191	5.06	0.067
Coefficient of thermal expansion, α, (1/°C)	1.17 x 10^{-5}	1.17 x 10^{-5}	1.7 x 10^{-5}	9.92 x 10^{-5}	0.0023 x 10^{-5}
Thermal conductivity, k, (W/m °C)	55.6	55.6	16.3	0.0415	0.03

Polypropylene and polyurethane foam were utilized as insulation layers for the SW and PIP systems, respectively. The lined pipeline featured a corrosion-resistant SS316L alloy liner. The present FE analysis assesses pipelines that are 5 m long. The outer and inner diameters of the single-layer pipeline are 0.152 m and 0.0796 m, respectively. The heat transfer coefficients for both the internal and external surfaces of the pipeline were computed based on fluid properties, the pipeline's diameter, and the velocities of the petroleum products and seawater.

The critical radius of insulation for PIP and SW pipelines is typically less than 0.1 mm. It is negligible compared to the insulation layer thickness due to the high external heat transfer coefficient. As a result, the critical radius of insulation was not considered in this analysis.

3. Finite Element Modeling

3.1 FE thermal buckling procedure

The finite element method (FEM) is commonly employed in analyzing the thermal buckling behavior of offshore pipelines. The methodology for combining steady-state heat transfer and nonlinear thermal buckling analyses is depicted in Fig. 3. This sequentially coupled analysis consists of four primary stages. In the first stage, a steady-state heat transfer analysis is conducted to calculate the temperature variation within the pipeline cross-section, utilizing convective heat transfer coefficients. In the second stage, the calculated temperature distribution is applied as a thermal load to a static structural analysis with fixed-end conditions, resulting in induced stresses within the pipeline (Moorthy et al., 2014). In the third stage, the stress distribution obtained from the static structural analysis is used as input for the following eigenvalue buckling analysis. Finally, the obtained mode shape is scaled and applied as an imperfection to the ideal pipeline to determine the real buckling temperature.

3.2 FE models and discretization

The 3D geometric models of the single-layer and multi-layer pipelines were developed using ANSYS DesignModeler. This numerical study uses FE models with 3D solid elements to investigate the thermal buckling behavior of imperfect submarine pipelines. The axisymmetric 3D pipeline models are discretized using 3D solid elements: SOLID90 and SOLID186 for simulation of their thermal and mechanical response. For static structural analysis, the element SOLID186 was utilized in place of SOLID90. The SOLID90 is a 20-noded temperature degrees of freedom element. The SOLID186 is a 20-node three-dimensional element with three displacement degrees of freedom (x, y, and z). It's good for advanced simulation-like situations related to large deformations, plastic strains, and nonlinear materials response (ANSYS, 2023). Its quadratic displacement variation suits complex deformations and hence yields better results than those of lower order elements. These components are based on non-linear shape functions, allowing a more precise representation of complex shapes and flexural actions. Furthermore, quadratic elements allow for a better approximation of curved edges and surfaces than linear elements, and are less sensitive to changes in the shape of the element.

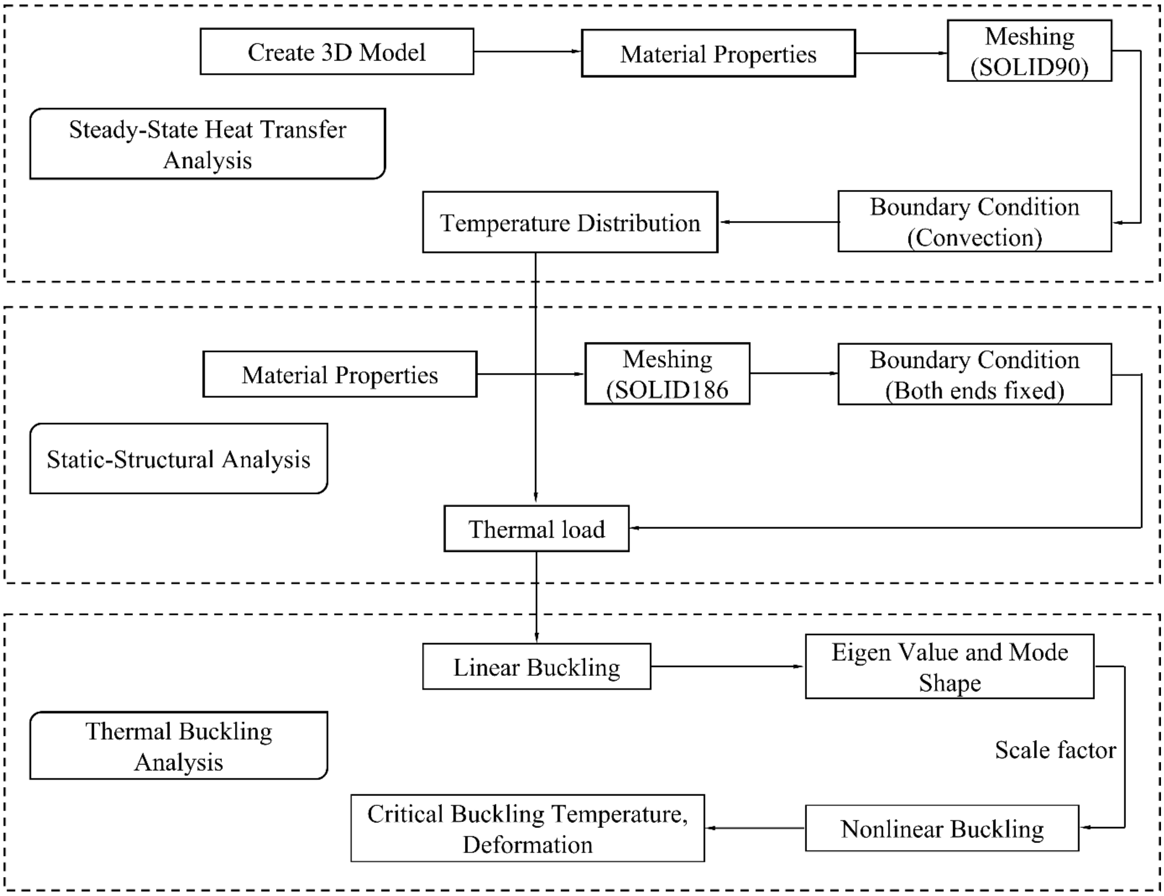

Fig. 3: Procedure for thermal buckling modeling

In this FE model, the insulation layers are bonded to the inner and outer pipes of the PIP and SW pipelines via bonded contact. Such bonded contact is for the purpose of preventing layers of the pipeline from sliding relative to one another. The contact among the layers is modelled with the ANSYS contact elements CONTA174 and TARGE170.

The temperature distribution obtained from the steady-state heat transfer analysis is then used as a thermal loading for the static structural analysis. Fixed boundary conditions are used to stabilize the pipeline by constraining the endpoints. This restriction prevents too much bending and decreases the chance of fatigue failure. This ensures its fixed end conditions control the pipeline response to dynamic loading, thus also suppressing resonance and other harmful effects. The fixed boundary conditions also provide strong seabed anchorage to avoid undesired displacement or movement by external forces like waves, currents, and seismic activity. Fixed conditions prevent any lateral displacement, keeping the pipeline in a straight line and minimizing stress concentrations. Without such restrictions, the pipeline itself could move or slide along the seabed because of water currents, variations in seabed topography, or external forces such as ship anchors or seismic activity. This would result in misalignment and generate stress, which eventually may raise the probability of a pipeline failure (Gamino et al., 2013; Phuor et al., 2023; Liu et al., 2014).

To simulate the actual boundary conditions, both ends of the pipeline are fully constrained using fixed supports in ANSYS, as depicted in Fig. 4. These boundary conditions completely restrict both the translational and rotational degrees of freedom at the specified locations, thereby preventing any movement or rotation in any direction.

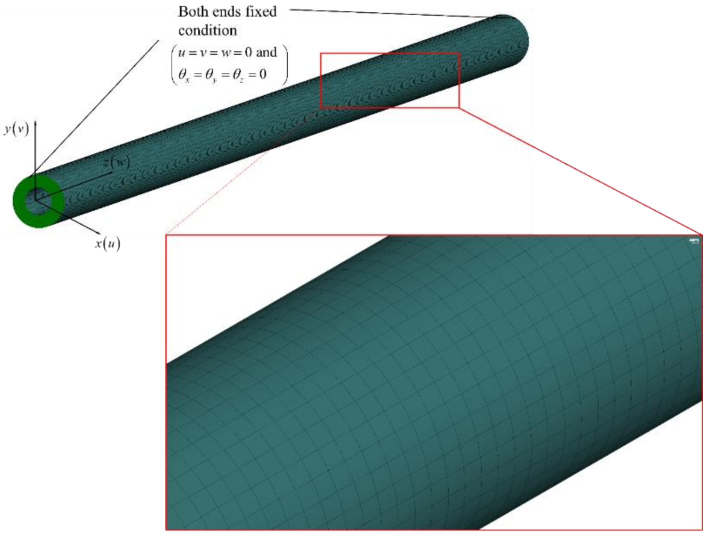

Fig. 4: Boundary conditions and Meshing

3.3 Eigenvalue buckling analysis

The eigenvalue buckling analysis method is useful for the preliminary determination of the critical buckling temperature of pipelines and can simplify the subsequent nonlinear buckling analysis. The static structural analysis produces results as inputs to an eigenvalue buckling analysis. The load multiplier as well as the mode shape of the pipeline are calculated in this analysis. The first one (with the lowest eigenvalue) is also used together with the highest temperature coming from the heat transfer analysis to assess the buckling temperature of the pipeline. This value gives meaningful implications, i.e., the maximum temperature where buckling takes place, and the corresponding mode shape (Chen et al., 2019).

3.4 Non-linear buckling analysis

The linear buckling analysis based on the perfectly elastic material response tends to overestimate the buckling temperature of a pipeline against the real application. This is because it fails to consider the effects of parameters as, initial imperfections, yielding of the material, and eccentricity of the load generated on the buckling itself. These effects bring about a lower failure temperature than the one predicted using linear analysis. For more accurate prediction, nonlinear buckling analysis is required. Initial imperfection pipe typically contains small imperfection or deviation from the perfect shape due to their can be manufacturing and installation processes. One of the most common and efficient approaches for processing pipeline (especially a cylindrical shell with uniform thickness) initial imperfection is the geometric imperfection analysis according to buckling modes. This technique consists in employing the overall deformation shape of one or a few modes of a linear buckling analysis that is scaled to simulate an initial imperfection. A nonlinear analysis is then carried out with this non-idealized geometry.

3.5 Mesh independence study

To ensure the accuracy of the calculated critical buckling temperature, a mesh-independence study was performed on the pipelines. This is because a finer mesh generally leads to more accurate FEA results. However, excessively fine meshes can significantly increase computational time without substantial improvements in accuracy. Therefore, it is crucial to carefully select an optimal mesh size to balance accuracy and efficiency in the design process. Fig. 5 illustrates the mesh independence study for the critical buckling temperature of a single-layer pipeline. The critical buckling temperature converged at a mesh size of 9 mm, corresponding to four elements across the pipeline thickness. This indicates that the single-layer pipeline buckles at a temperature of 252.54°C under linear buckling analysis.

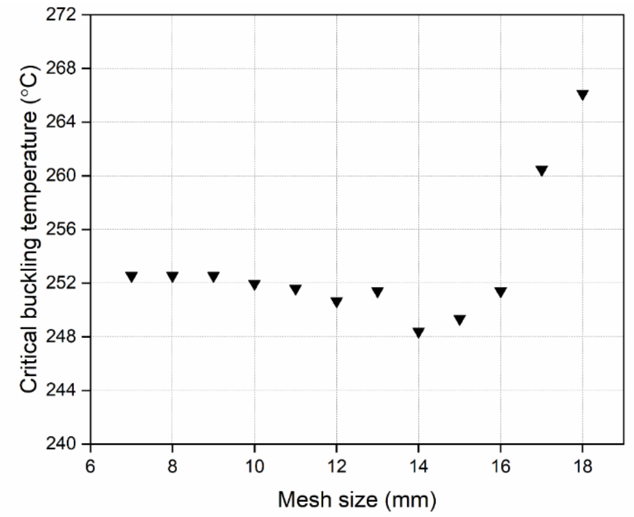

Fig. 5: Mesh independence study

4. Results and Discussion

4.1 Temperature distribution

Fig. 6 illustrates the temperature variation across the radius of both single-layer and multilayer pipelines. Steady-state heat transfer analysis indicates that both single-layer and lined pipelines exhibit comparable peak temperatures, reaching approximately 4.8°C. In contrast, PIP and SW pipelines demonstrate significantly higher peak temperatures, attaining approximately 60°C and 55°C, respectively. This represents an approximately 12 times increase in peak temperature for PIP and SW pipelines compared to the single-layer and lined configurations. The outer pipes experience a temperature of approximately 4.2°C, which is the same as the environmental or seawater temperature.

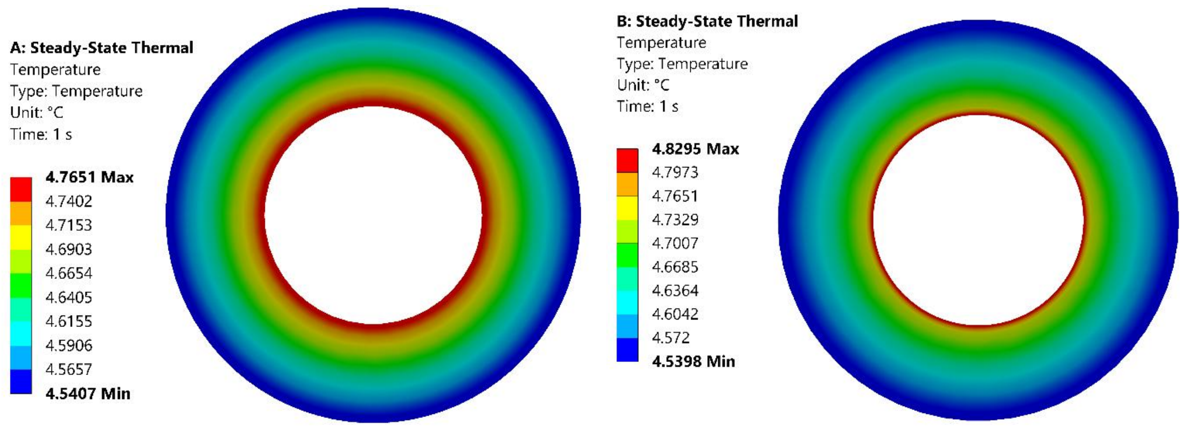

(a) Single-layer pipeline (b) Lined pipeline

Fig. 6.1: Pipelines' temperature distribution (a & b)

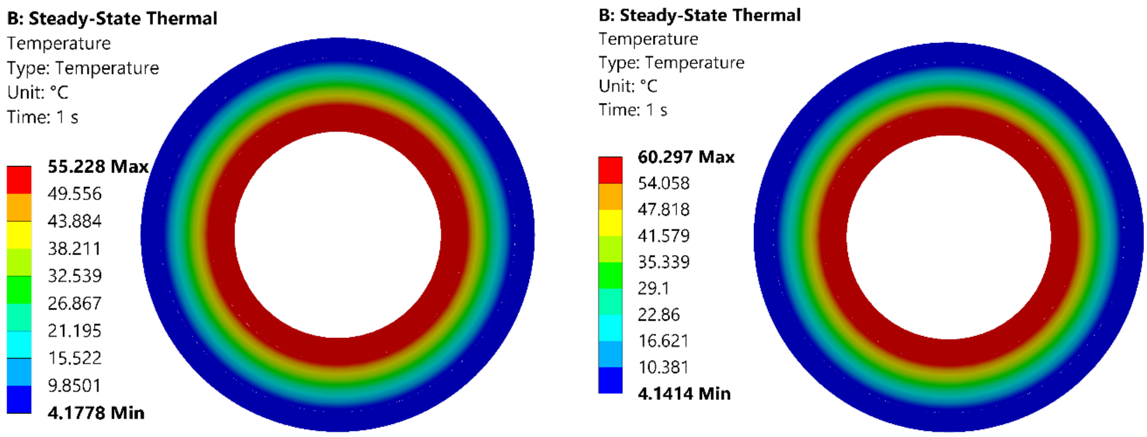

(c) SW pipeline (d) PIP

Fig. 6.2: Pipelines' temperature distribution (c & d)

Fig. 7 illustrates the temperature distribution across all the aforementioned pipeline radii. It clearly shows that the maximum temperature occurs at the inner layer of all pipeline configurations, as indicated by the steady-state heat transfer analysis. The temperature gradually decreases from the inner to the outer layer for both single-layer and lined pipelines. Due to high convective heat transfer, the inner layer temperature closely matches the ambient temperature. As a result, insulation is essential to mitigate the risk of paraffin and hydrate accumulation. The lined pipeline exhibits more significant temperature changes within the inner liner layer than in the outer layer. In SW and PIP pipelines, the temperature decreases logarithmically across the insulation layers as the radius increases.
The SW and PIP systems exhibit relatively constant temperature profiles within their inner and outer layers, attributable to their superior thermal conductivity. Conversely, the insulating layers, especially in the PIP system, demonstrate a steeper temperature gradient. This suggests that the insulation effectively mitigates heat transfer between the inner and outer surfaces, resulting in a significant temperature differential across the pipeline's radial direction.

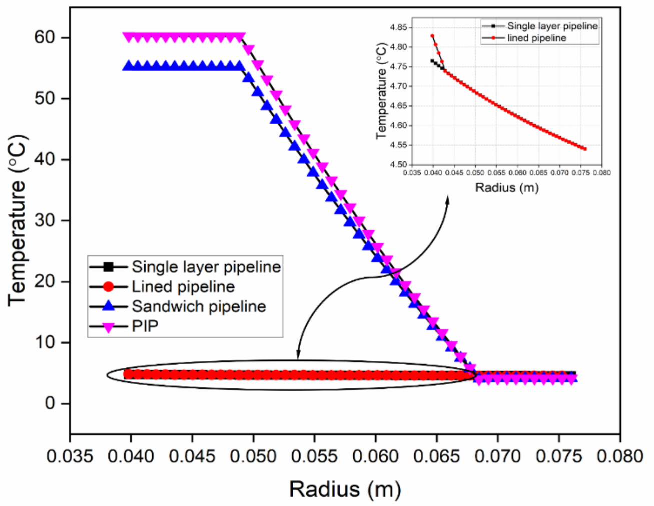

Fig. 7: Radial temperature gradients in multilayer pipelines

Fig. 8 presents the curve fit for the temperature variation across the radii of both the single-layer and insulation layer of the SW pipelines.

Similarly, as shown in Fig. 8(b), the temperature variation within the insulation layer follows a logarithmic pattern due to steady-state heat transfer between the inner and outer layers of the pipeline.

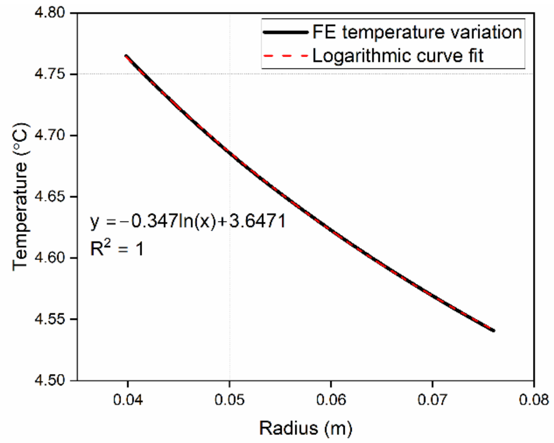

(a) Singe layer pipeline

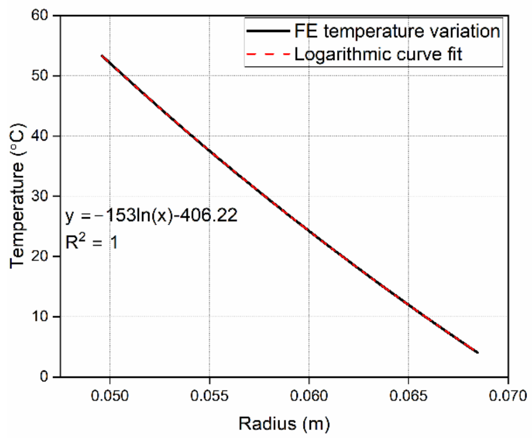

(b) SW pipeline - Insulation layer

Fig. 8: Logarithmic variation of temperature in pipelines

4.2 von Mises stress variation

When dealing with a pipeline with a non-homogeneous cross-section, such as a PIP or multilayer pipeline, it is crucial to analyze the stress distribution across the radial direction. To achieve this numerically, a static structural analysis should be conducted, assuming the linear behavior of both the pipeline and the materials involved. This approach helps to accurately predict the stress patterns and ensure the pipeline's structural integrity under various conditions.

Fig. 9 illustrates the variations in von Mises stresses across the radius of the pipelines. In single-layer pipeline, the stress decreases with the radius because of radial temperature-decreased, and this effect has a direct influence on stress. The lined pipeline, however, has a tremendous change in stress because the temperature drops steeply at the radius of the liner, penetrating into the liner material. In particular, the stress decreases much faster than to the liner radius than the flow behind the liner. Insulating layers (PIP and SW) were subjected to much less stress state than the steel layers, particularly due to very low modulus of elasticity.

There are several factors contributing to the stress distributions in the PIP and SW pipes, such as the temperature difference across the pipes, the modulus of elasticity values of the materials, and also the corresponding thermal expansion coefficients. They also cause axial bending stress in the pipe, which changes with the radial position in the pipeline. Because the outer layer of the pipeline is at a greater distance from the neutral axis, it has a greater bending stress than the inner and insulation layers. The higher temperature difference between the inner and outer pipes of the SW pipeline, and direct relation of the temperature with the thermal expansion coefficient, means that the elongation of the inner pipe and its insulation layer is also greater than that of the outer pipe.

As a result, the inner pipe undergoes compressive stress, inducing lateral buckling of the outer pipe. In addition to temperature fluctuations, the material's Poisson's ratio can also influence stress variations within the pipeline. Overall, these factors culminate in maximum stress in the outer pipe of the SW pipeline, whereas the insulation layer undergoes reduced stress. As the pipeline's temperature varies, it undergoes thermal expansion or contraction, influenced by its coefficient of thermal expansion. Discrepancies in the linear thermal expansion coefficients of the pipeline's layers can lead to stress development in neighboring layers due to differential expansion or contraction. The stress distribution within lined, SW, and PIP pipelines is characterized by significant gradients, particularly at layer interfaces where abrupt temperature changes occur. In PIP systems, the higher temperature profile, the high Young's modulus of the inner pipe material, and particularly the low coefficient of thermal expansion of the insulation layer contribute to higher stress in the inner pipe. Conversely, the insulation layer's low coefficient of thermal expansion and low Young's modulus result in lower stress.

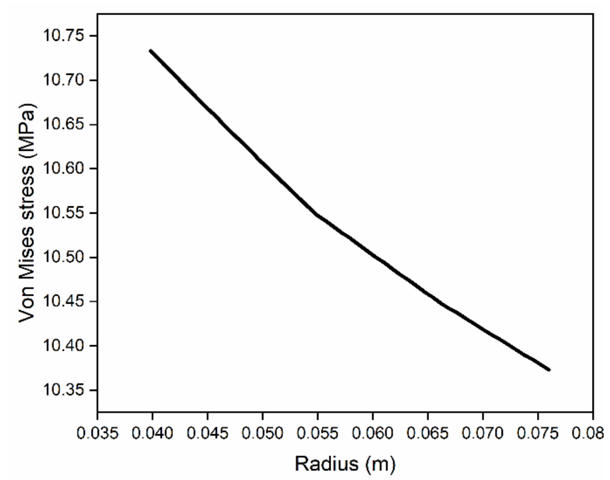

(a) Single-layer pipeline

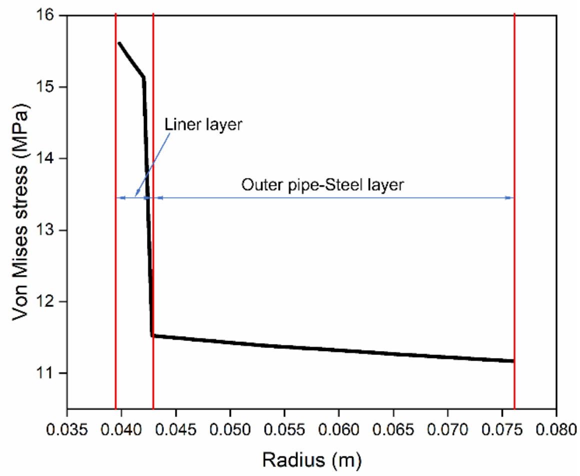

(b) Lined pipeline

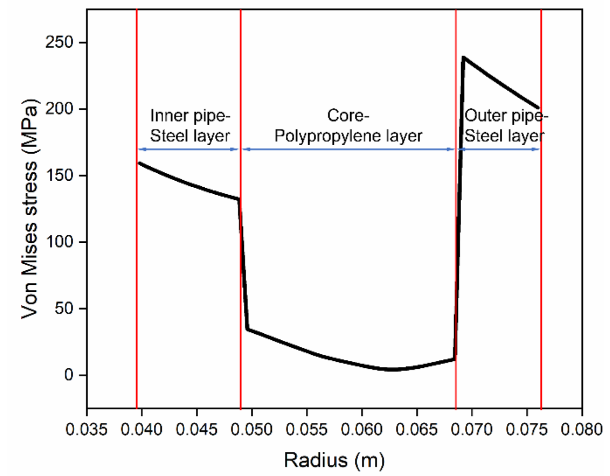

(c) SW pipeline

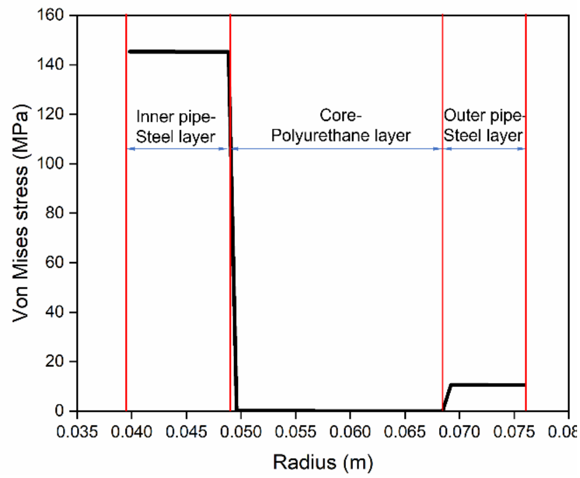

(d) PIP

Fig. 9: Stress profiles along the radius of the pipelines

As the temperature falls from approximately 60°C to 4°C, the outer pipe in the PIP system contracts considerably more than both the inner pipe and the insulation layer. This disparity in contraction leads to compressive stress in the inner pipe and tensile stress in the outer pipe. The insulation layer's low elastic modulus, in comparison to steel, limits its impact on the overall stress distribution. As a result, the inner pipe experiences greater stress than the outer pipe. Static structural FE modeling demonstrated that the SW pipeline was subjected to higher stress levels than the PIP. This implies that the insulating material in the SW pipeline contributes to both thermal insulation and structural integrity.

4.3 Critical buckling temperature

Fig. 10 depicts the effect of imperfection on the buckling temperature of both single-layer and multilayer pipelines. Both single-layer and lined pipeline configurations exhibited nearly isothermal steady-state thermal profiles, with peak temperatures reaching approximately 4.8°C. The nonlinear thermal buckling FE analysis determined buckling temperatures of 230°C for the single-layer and 224°C for the lined pipeline, as illustrated in Fig. 10 (a, b). The buckling temperature obtained from the nonlinear analysis with a 5% scale factor was 9% and 10% lower than the eigenvalue buckling critical temperature. Introducing a 3 mm corrosion-resistant liner to the single-layer pipeline did not alter its buckling temperature, which remained in the range of 230°C to 220°C. The single-layer pipelines exhibit a simpler thermal buckling mechanism compared to PIP and SW pipelines. The latter two configurations exhibit more intricate buckling behavior due to the interplay between multiple layers. As depicted in Fig. 9, SW and PIP systems demonstrate a significantly greater temperature gradient across their thickness relative to single-layer and lined pipelines. This disparity in temperature distribution directly influences the buckling temperature of PIP and SW pipelines. The temperature gradients within the insulation layer of a pipeline can significantly influence its critical buckling temperature. This effect is more pronounced in multi-layer pipelines, such as SW and PIP systems, compared to single-layer pipelines. The insulation layers in these pipelines result in varying axial compressive forces along the pipeline's length. The steady-state heat transfer analysis reveals that SW and PIP systems reach maximum temperatures of approximately 55°C and 60°C, respectively. As a result, these pipelines exhibit significantly higher buckling temperatures in the nonlinear thermal buckling analysis, reaching 377°C and 501°C, respectively, as shown in Fig. 10 (c, d). The low thermal expansion coefficient of the core layer in the PIP system further enhances its buckling resistance.

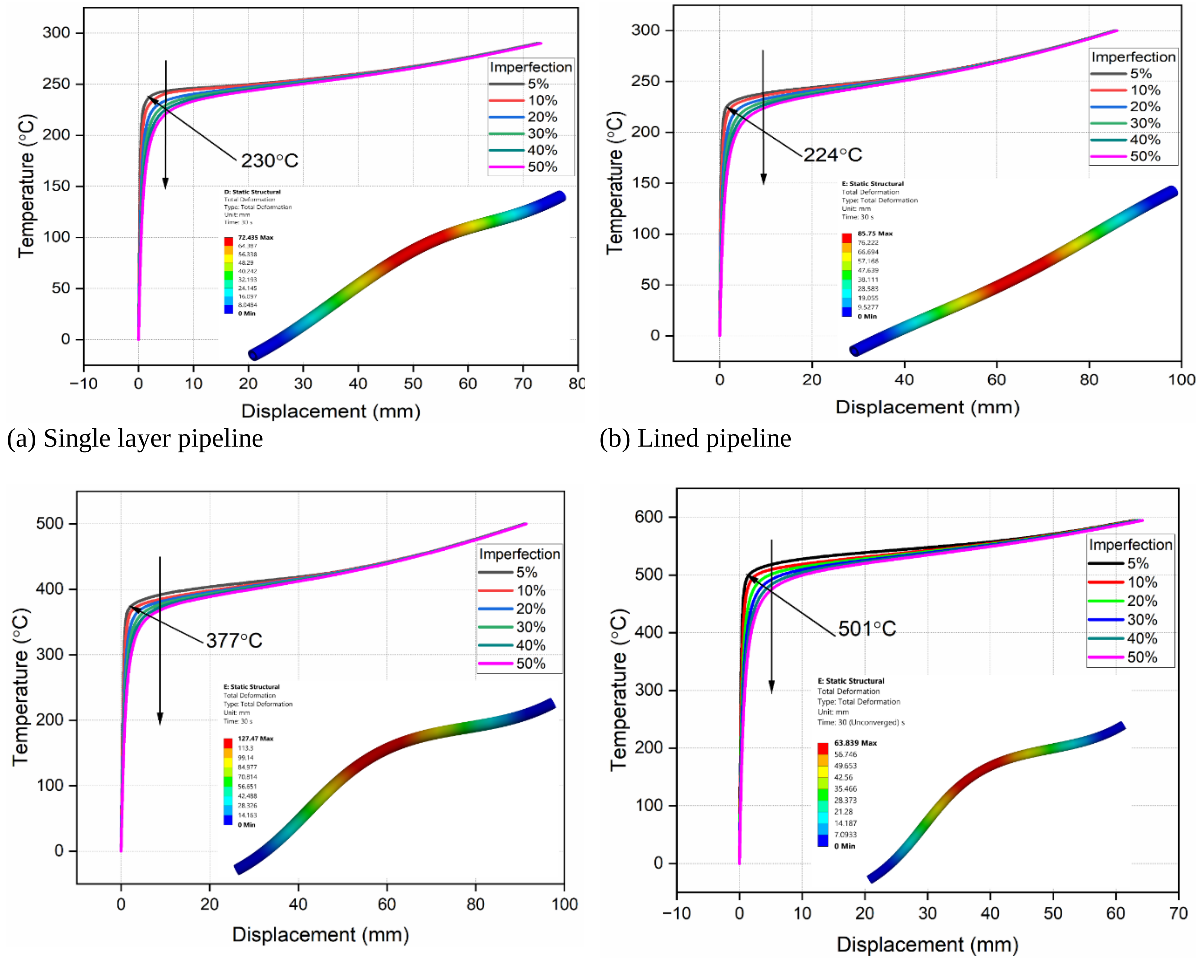

(a) Single layer pipeline (b) Lined pipeline

(c) SW pipeline d) PIP

Fig. 10: Effect of imperfection on buckling temperature

As illustrated in Fig. 10, the nonlinear buckling analysis demonstrates that introducing geometric imperfections in pipeline structures reduces their buckling temperature. Specifically, the critical buckling temperature of these pipelines inversely correlates with the magnitude of the initial imperfections. The initial imperfections in a pipeline significantly reduce the critical buckling temperature by creating stress concentrations, disrupting the uniform stress distribution, acting as initiation points for buckling, and amplifying the deformations. These imperfections cause localized deformations and stresses that make the pipeline more prone to buckling at lower temperatures. Consequently, the imperfections lower the structural integrity of the pipeline, reducing the critical buckling temperature and promoting earlier failure under thermal stresses. The comparison of critical buckling temperatures computed from nonlinear and linear thermal buckling analyses is shown in Fig. 11. It clearly indicates that, for the 5% scale factor initial imperfection, the buckling temperatures of single-layer and multilayer pipelines are lower than the linear eigenvalue buckling temperature. This trend holds true for all simulated scale factors, including 10%, 20%, 30%, 40%, and 50%.

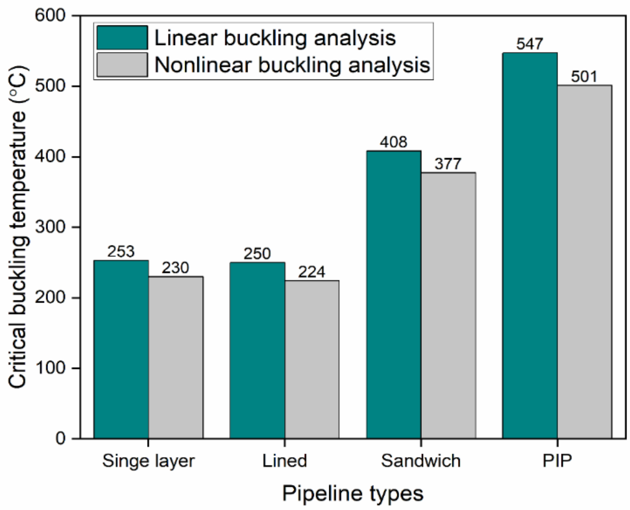

Fig. 11: Critical buckling temperature comparison

5. Conclusions

The present study uses non-linear FE modeling to investigate the impact of initial imperfection and temperature variation along the radial direction on the buckling temperature of multilayer pipelines, specifically lined, PIP, and SW pipelines. The variations in temperature and stress profiles across the radius and each pipeline type's buckling temperature are analyzed. The buckling temperatures calculated from the nonlinear buckling analyses of these pipelines are compared with those of a standard single-layer pipeline. The main conclusions of this numerical study are as follows:

- The steady-state heat transfer analysis reveals that the maximum temperatures of both single-layer and lined pipelines are nearly identical to the environmental temperature, which is below the wax appearance temperature. Consequently, the inclusion of insulation layers is crucial for offshore pipeline design.
- The FE results show that the temperature distribution along the radius of the inner and outer pipes of PIP and SW pipelines is nearly uniform. Conversely, the temperature gradient across the insulation layer decreases logarithmically as the radial distance increases.
- The PIP and SW pipelines show distinct stress patterns across their radial dimensions. The outer pipe of the SW system endures the maximum stress, while the inner pipe of the PIP system is subjected to the highest stress. Nonetheless, both pipeline configurations exhibit very low or insignificant stress variation along the radius of the insulation layers. In overall comparison, the SW pipeline undergoes higher stress than the PIP system.
- The FE analysis results indicate that the lined pipeline's buckling resistance is virtually indistinguishable from that of a single-layer pipeline.
- The PIP system demonstrates the highest buckling resistance among all pipelines evaluated, exhibiting a critical buckling temperature of 501°C. This represents a substantial 33% improvement over the SW pipeline and a notable 118% improvement compared to the single-layer pipeline.
- Eigenvalue buckling analysis consistently overpredicts the critical buckling temperature for all pipelines compared to nonlinear buckling analysis. This is attributed to the inherent limitation of eigenvalue analysis in neglecting the influence of initial geometric imperfections, which significantly impact the buckling behavior of pipelines.
- The nonlinear buckling results reveal that the introduction of geometric imperfections in pipeline systems can reduce the critical temperature for buckling
- The critical buckling temperature of pipelines is negatively impacted by the magnitude of initial imperfections, as an increase in imperfections leads to a decrease in the critical buckling temperature.

Consequently, the buckling temperature of the pipelines is significantly influenced by the properties of the insulation layers, the temperature distribution across the pipeline radius, and the presence of imperfections in the pipelines.

References

Aiyejina, A., Chakrabarti, D.P., Pilgrim, A. and Sastry, M.K.S. (2011): Wax formation in oil pipelines: A critical review. International Journal of Multiphase Flow, Vol. 37, No. 7, pp. 671-694. https://doi.org/10.1016/j.ijmultiphaseflow.2011.02.00

Andreuzzi, F. and Perrone, A. (2001): Analytical solution for upheaval buckling in buried pipeline. Computer Methods in Applied Mechanics and Engineering, Vol. 190, No. 39, pp. 5081-5087. https://doi.org/10.1016/S0045-7825(00)00366-2

ANSYS 23.0 Release, ANSYS, Inc., 275 Technology Drive, Canonsburg, PA 15317

Bracaglia, F., Masia, R., Pagani, A., Zappino, E. and Carrera, E. (2024): Thermal buckling of variable stiffness composite laminates using high order plate finite elements. Composite Structures, Vol. 345, 118393. https://doi.org/10.1016/j.compstruct.2024.118393

Castello, X. and Estefen, S. F. (2008): Sandwich pipes for ultra-deep-water applications, Offshore Technology Conference, OTC-19704-MS, Texas, U.S.A. https://doi.org/10.4043/19704-MS

Chakraborty, S., Talimi, V., Muzychka, Y. and McAffee, R. (2016): Modeling of heat loss from offshore buried pipeline through experimental investigations and numerical analysis. In OTC Arctic Technology Conference (pp. OTC-27419). OTC.

Chen, W., Wan, F., Guan, F., Liu, X., Yang, Y. and Zhou, C. (2024): The effect of seabed flexibility on the impact damage behavior of submarine sandwich pipes. Applied Ocean Research, Vol. 142, 103838. https://doi.org/10.1016/j.apor.2023.103838

Chen, Z., Yi, Y. B., Bao, K. and Zhao, J. (2019): Numerical analysis of the coupling between frictionally excited thermoelastic instability and thermal buckling in automotive clutches, Proceedings of the Institution of Mechanical Engineers, Part J: Journal of Engineering Tribology, Vol. 233, No. 1, pp. 178-87. https://doi.org/10.1177/1350650118772664

Cornacchia, F., Liu, T., Bai, Y. and Fantuzzi, N. (2019): Tensile strength of the unbonded flexible pipes. Composite Structures, Vol. 218, pp.142-151. https://doi.org/10.1016/j.compstruct.2019.03.028

De Leeuw, L.W., Diambra, A., Kwon, O.S. and Sextos, A. (2022): Modulating pipe-soil interface friction to influence HPHT offshore pipeline buckling, Ocean Engineering, Vol. 266, 112713. https://doi.org/10.1016/j.oceaneng.2022.112713

Du, F., Li, C. and Wang, W. (2023): Development of Subsea Pipeline Buckling, Corrosion and Leakage Monitoring. Journal of Marine Science and Engineering, Vol. 11, No. 1, 188. https://doi.org/10.3390/jmse11010188

Estefen, S.F., Netto, T.A. and Pasqualino, I.P. (2005): Strength analyses of sandwich pipes for ultra deepwaters. Journal of Applied Mechanics, Vol. 72, No. 4, pp. 599-608. https://doi.org/10.1115/1.1940667

Gamino, M., Abankwa, S. and Pascali, R. (2013): FSI methodology for analyzing VIV on subsea piping components with practical boundary conditions. Proceedings of the ASME 2013 32nd International Conference on Ocean, Offshore and Arctic Engineering. Volume 7: CFD and VIV. Nantes, France. June 9–14, 2013. V007T08A028. ASME. https://doi.org/10.1115/OMAE2013-10419

Gavriilidis, I. and Karamanos, S.A. (2019): Bending and buckling of internally-pressurized steel lined pipes. Ocean Engineering, Vol. 171, pp. 540-553. https://doi.org/10.1016/j.oceaneng.2018.11.052

Guo, L. P., Run, L. and Yan, S. W. (2013): Global buckling behaviour of submarine unburied pipelines under thermal stress, J. Cent. South Univ., Vol. 20, pp. 2054-65. https://doi.org/10.1007/s11771-013-1707-4

Hobbs, R. E. (1984): In-service buckling of heated pipelines, J.Transp.Eng., Vol. 110, No. 2, pp. 175-89. https://doi.org/10.1061/(ASCE)0733-947X(1984)110:2(175)

Janna, W.S. (2018): Engineering heat transfer. CRC press.

Kumar, K., El Mohtar, C. and Gilbert, R (2022): Conductive and convective heat transfer in inductive heating of subsea buried pipelines. Journal of Pipeline Systems Engineering and Practice, Vol. 13, No. 4, 04022031. https://doi.org/10.1061/(ASCE)PS.1949-1204.0000672

Liang, K., Yin, Z. and Hao, Q. (2024): A reduced-order method for geometrically nonlinear analysis of the wing-upper-skin panels in the presence of buckling. Computers & Mathematics with Applications, Vol. 170, pp. 42-55. https://doi.org/10.1016/j.camwa.2024.06.014

Liu, R., Xiong, H., Wu, X. and Yan, S. (2014): Numerical studies on global buckling of subsea pipelines. Ocean Engineering, Vol. 78, pp. 62-72. http://dx.doi.org/10.1016/j.oceaneng.2013.12.018

Govindaraj, M., Murthy, H. N., Patil, S., Sudarsan, K.,Nandokumar, O.R, Kumar, A. K., and Munishaiah, K. (2014): Buckling behaviour of underwater vessels by experimental, numerical and analytical approaches, Journal of Naval Architecture and Marine Engineering, Vol. 11, No. 1, pp. 15-28. http://dx.doi.org/10.3329/jname.v11i1.16087

Ning, J., Liu, S., Lin, T. and Huang, W. (2022): Pipeline element for upheaval buckling analysis of submarine pipelines with geometric-imperfections under high temperature high pressure. Ocean Engineering, Vol. 264, 112456. https://doi.org/10.1016/j.oceaneng.2022.112456

Onyegiri, I. and Kashtalyan, M. (2017): Finite element analysis of a sandwich pipe joint. Ocean Engineering, Vol. 46, pp. 363-374. https://doi.org/10.1016/j.oceaneng.2017.09.042

Park, D.S., Shin, M.B. and Seo, Y. K. (2020): Heat-transfer characteristics of subsea pipelines embedded in multilayered soils. SPE Journal, Vol. 25, No. 3, pp.1128-1139. https://doi.org/10.2118/199353-PA

Phuor, T., Trapper, P.A. and Ganz, A. (2023): An Analytical Expression for the Fundamental Frequency of a Long Free-Spanning Submarine Pipeline. Mathematics, Vol. 11, No. 21, pp. 4481. https://doi.org/10.3390/math11214481

Shadravan, A. and Amani, M. (2012): HPHT 101-what petroleum engineers and geoscientists should know about high pressure high temperature wells environment. Energy Science and Technology, Vol. 4, No. 2, pp. 36-60.

Song, K., Choi, Y., Park, G., Cho, N.K. and Kim, C.S. (2022): Study on cyclic plastic behaviour of sandwich pipelines subjected to cyclic thermo-mechanical loads. Ocean Engineering, Vol. 257, 111622. https://doi.org/10.1016/j.oceaneng.2022.111622

Swain, B. K., Sahu, S., Ojha, K. L., and Dash, G. C. (2023): Heat transfer with viscous dissipation and entropy generation in a nanofluid flow through a porous medium. Journal of Naval Architecture and Marine Engineering, Vol. 20, No. 2, pp. 127-142.

Tafreshi, R., Khan, Z., Franchek, M. and Grigoriadis, K. (2015). Two-phase heat transfer modeling in subsea pipelines. In: Fathi, M. (eds) Integrated Systems: Innovations and Applications. pp.243-256. Springer, Cham. https://doi.org/10.1007/978-3-319-15898-3_15

Taylor, N. and Tran, V. (1996): Experimental and theoretical studies in subsea pipeline buckling. Marine Structures, Vol. 9, No. 2, pp. 211-257. https://doi.org/10.1016/0951-8339(94)00021-J

Vazouras, P., Tsatsis, M. and Dakoulas, P. (2021): Thermal upheaval buckling of buried pipelines: Experimental behavior and numerical modelling, J. Pipeline Syst. Eng. Pract., Vol. 12, No. 1, 04020057. https://doi.org/10.1061/(ASCE)PS.1949-1204.0000507

Vedeld, K., Osnes, H. and Fyrileiv, O. (2012): Analytical expressions for stress distributions in lined pipes: Axial stress and contact pressure interaction. Marine Structures, Vol. 6, No. 1, pp. 1-26. https://doi.org/10.1016/j.marstruc.2011.12.003

Wang, S., Li, L., Wu, W., Wang, T. and Liu, H. (2023): Analytical Study of Lateral Buckling of Pipelines with Initial Imperfection Based on Fixed-Fixed Beam Model. Applied Sciences, Vol, 13, No. 5, 3227. https://doi.org/10.3390/app13053227

Wang, X., Yuan, L., Xu, P., Ding, Z., Wang, Y. and Gong, S. (2024): Evaluation of dynamic behaviour of pipe-in-pipe systems for deepwater J-lay method. Applied Ocean Research, Vol 53, 104229. https://doi.org/10.1016/j.apor.2024.104229

Wang, Y., Wei, N., Wan, D., Wang, S. and Yuan, Z. (2019): Numerical simulation for preheating new submarine hot oil pipelines. Energies, Vol. 12, No. 18, 3518. https://doi.org/10.3390/en12183518

Wang, Y., Zhang, X., Zhao, Y., Chen, H., Duan, M. and Estefen, S.F. (2017): Perturbation analysis for upheaval buckling of imperfect buried pipelines based on nonlinear pipe-soil interaction. Ocean Engineering, Vol. 132, 92-100. https://doi.org/10.1016/j.oceaneng.2017.01.022

Wang, Z., Tang, Y., Yang, J. and Soares, C.G. (2020): Analytical study of thermal upheaval buckling for free spanning pipelines. Ocean Engineering, Vol. 218, 108220. https://doi.org/10.1016/j.oceaneng.2020.108220

Wagner, H.N.R. and Hühne, C. (2025): On the imperfection sensitivity and design of buckling critical wind turbine towers. Thin-Walled Structures, Vol. 206, 112577. https://doi.org/10.1016/j.tws.2024.112577

Wei, H., Dong, S., Xu, L., Zhao, J., Ma, Y. and Zhang, H. (2024). The influence of the outer pipe during internal MFL detection in subsea steel pipe-in-pipe. Journal of Magnetism and Magnetic Materials, Vol. 600, 172149. https://doi.org/10.1016/j.jmmm.2024.172149

Xu, L. and Lin, M. (2017): Numerical study on critical axial forces of upheaval buckling for initially stressed submarine pipelines on uneven seabed. Ocean Engineering, Vol. 145, 344-358. https://doi.org/10.1016/j.oceaneng.2017.09.013

Yang, Y., Wan, F., Guan, F., Tian, H. and Chen, W. (2024): Buckling behavior of sandwich pipe under external pressure and lateral load. International Journal of Pressure Vessels and Piping, Vol. 207, 105114. https://doi.org/10.1016/j.ijpvp.2023.105114

Yu, J., An, C., Tang, Q., Zhang, J. and Zhang, Y. (2024): Heat transfer characteristics of subsea long-distance pipeline subject to direct electrical heating. Geoenergy Science and Engineering, Vol. 234, 212679. https://doi.org/10.1016/j.geoen.2024.212679

Yu, J., Xu, W., Chen, N.Z., Jiang, S., Xu, S., Li, H. and Han, M. (2022): Effect of dent defects on the collapse pressure of sandwich pipes. Thin-Walled Structures, Vol. 170, 108608. https://doi.org/10.1016/j.tws.2021.108608

Zhang, F., Ma, Y. and Yin, H. (2014): Determination of the thermal exchange coefficient between subsea soil and buried submarine pipeline. In ICPTT 2014: Creating Infrastructure for a Sustainable World, pp. 276-282. https://doi.org/10.1061/9780784413821.031

Zhang, X., Duan, M. and Soares, C.G. (2018): Lateral buckling critical force for submarine pipe-in-pipe pipelines. Applied Ocean Research, Vol. 78, pp. 99-109. https://doi.org/10.1016/j.apor.2018.06.007

Zhang, Z., Liu, H. and Chen, Z. (2019): Lateral buckling theory and experimental study on pipe-in-pipe structure. Metals, Vol. 9, No. 2, 185. https://doi.org/10.3390/met9020185